DSP Methods for Correcting Dispersion and Pulse Width Effects During Pulsed Wire Measurements*

Matthew Kasa

Advanced Photon Source
Argonne National Laboratory
Lemont, Illinois, U.S.A.
kasa@aps.anl.gov

Jafar Saniie

Department of Electrical and Computer Engineering
Illinois Institute of Technology
Chicago, Illinois, U.S.A.
saniie@iit.edu

***Abstract*— Measuring a magnetic field by pulsing electrical current through a wire placed in the magnetic field, then measuring the displacement of the wire as a travelling wave passes a displacement sensor is a technique typically referred to as a pulsed wire measurement. The techniques presented provide a method of correcting for the dispersion in the travelling wave and the averaging effects of pulse duration. The methods used to implement the correction algorithm of dispersion are based on allpass filtering design techniques that allow the filter parameters to be modified on-the-fly. Correction of errors introduced by the pulse width duration is performed by utilizing deconvolution. The algorithm is described and measurement results are presented.**

Keywords—Pulsed wire, dispersion correction, magnet measurement

I. Introduction

The pulsed wire measurement technique is implemented by pulsing electrical current through a wire placed in the magnetic field, and then measuring the displacement of the wire as a travelling wave passes a displacement sensor. It was originally proposed by Warren in 1988 [1] and has been explored by others since [2] [3] [4] [5]. Pulsed wire measurements are taken by positioning and tensioning a thin conducting wire through the region of interest of a magnet and sending an electrical pulse through the wire. Then measuring the wire displacement as a function of time at a location on the wire outside the magnetic field. The goal of these measurements is to extract the magnetic field distribution of the magnet from the time dependent wire displacement data.

Some challenges of the pulsed wire technique include dispersion of the traveling wave's frequency components due to stiffness of the wire, averaging effects caused by the duration of the pulsed current, sag of the stretched wire, and undesired motion of the wire from environmental factors such as floor vibration and air circulation. An algorithm for correcting the measured signal due to the effects of dispersion and the width of the current pulse has been demonstrated by Arbelaez et. al. [4]. The techniques presented here provide an alternate method of correction for the dispersion in the travelling wave, and the averaging effects of pulse duration. The main benefit of the method presented to correct for dispersion is the flexibility of the technique and the ability to modify its characteristics during signal processing.

* Work supported by the U.S. Department of Energy, Office of Science, under Contract No. DE-AC02-06CH11357.

II. The Travelling Wave

When current is present in the wire, the wire experiences a force that causes it to be displaced wherever the magnetic field is present, thus creating an identical pair of travelling waves, each representing the integral of the magnetic field. One travels in the positive z-direction and the other in the negative z-direction. Derivations of the solution of the wave equation for the pulsed wire scenario have been determined using different methods, and can be found in [1] [3] [4].

A. Dispersion

In an ideal situation, all frequency components of the travelling wave travel down the wire at the same velocity. In the real case, the stiffness of the wire causes higher frequency components to travel down the wire at a faster speed than the lower frequency components; referred to as dispersion.

If the wire has a radius r then then $M = \pi r^4/4$. Following the analysis in [7] [8] the frequency dependent wave speed formula can be approximated as

$$c(\omega) = c_0\left(1 + a\frac{EM\omega^2}{2Tc_0^2}\right) \quad (1)$$

where E is Young's modulus, M is the area moment of inertia of the wire, T is the tension of the wire, c_0 is the wave velocity and a is the term used to fit the analytical equation to the measured data.

B. Pulse Width Moving Average

The pulse width of the current needs to have a finite duration which has the effect of averaging the first integral over the length of the pulse. If the shape of the current as a function of time is a rectangular pulse this can be thought of as a moving average convolution of the first integral of the magnetic field during a short pulse. If the field does not significantly change over the distance, $c_0\Delta t$, where Δt is the pulse width, then the averaging effect is negligible.

III. Correction

A. Wave Speed Measurement

A common technique of performing two experimental measurements, presented here as well as in [4], is used to

978-1-5386-3383-0/17/$31.00 ©2017 IEEE

measure the wave speed as a function of frequency. The technique requires two measurements of the wire displacement as a function of time, u_1 and u_2, where u_2 is a measurement with a greater distance between the magnet and sensor. The change in the distance between the sensor and magnet of the two measurements is Δz. If the two measurements are transformed into the frequency domain by the Fourier transform, becoming U_1 and U_2, and the conjugate of U_1 is multiplied with U_2, assuming the magnitudes of the transformations are the same, the result is

$$U_1^* U_2 = |U|^2 e^{i(\varphi_2 - \varphi_1)} \tag{2}$$

Using the time shifting property of the Fourier transform, the effect of shifting the measurement location by Δz is a phase shift in the frequency domain equivalent to $\varphi = \frac{\omega}{c}\Delta z$. Using this fact and the phase of (2) the following relationship is established to yield the wave speed as a function of frequency

$$c(\omega) = \frac{\omega}{(\varphi_2 - \varphi_1)}\Delta z \tag{3}$$

The result of (3) can then be compared to the analytical equation of the wave speed shown in (1). The scaling parameter, a, can be used to fit the analytical equation to the measured data.

B. Dispersion Correction

Dispersion of the traveling wave occurs because the wave speed is a non-linear function of frequency. The non-linearity of the problem does not allow for Fourier analysis to be performed. The method presented here addresses this issue and is based on a digital filtering method presented by Abel and Smith [6]. Their method uses digital allpass filters that can be cascaded together to create a high order filter that does not suffer from numerical difficulties and results in a robust and flexible design. The design method creates a filter that can match a prescribed group delay as a function of frequency. In addition, the filter coefficients that control the prescribed group delay can be recalculated and updated during the processing of the signal.

So as not to create confusion between the dimensional z coordinate and the discrete time z-transform notation used in digital signal processing, $\tilde{z}$ will be used to represent the z-transform. A first order allpass filter, consisting of one pole and one zero in the complex frequency domain is represented by the transfer function

$$G(z) = \frac{-\rho e^{j\theta} + \tilde{z}^{-1}}{1 - \rho e^{j\theta}\tilde{z}^{-1}} \tag{4}$$

where θ is the normalized frequency with π being the Nyquist frequency, and ρ represents the amount of group delay in samples. In the $\tilde{z}$-plane the transfer function has a pole inside the unit circle at radius ρ and angle θ, and the zero of the transfer function is at the same angle θ, but at a radius of $1/\rho$.

The group delay of a filter is defined as the negative derivative of the phase response with respect to frequency, $d\varphi(\omega)/d\omega$. In the case of the allpass filter the group delay is

$$\tau(\omega) = \frac{1-\rho^2}{1+\rho^2 - 2\rho\cos(\omega - \theta)} \tag{5}$$

and the delay is maximum at the pole frequency, θ, and is

$$\max\{\tau(\omega)\} = \frac{1+\rho}{1-\rho} \tag{6}$$

So, the group delay increases as the pole approaches the unit circle and decreases as the pole approaches the origin. Also, the integral of the group delay around the unit circle is always 2π.

For the pulsed wire measurement, the wave speed described in (3) can be used to define the desired group delay, $\delta(\omega)$. The group delay at a distance z from the sensor is

$$\delta(\omega) = \frac{d}{d\omega}\left(\omega \frac{max\{z\}}{c_0} - \omega \frac{\Delta z}{c(\omega)}\right) \tag{7}$$

where $\max\{z\}$ is greater than the distance from the sensor to the end of the magnet. It is important to mention that due to assumptions and simplifications made during the forming of (1), it is valid over a range of frequencies $\omega < \frac{2\pi c_0}{10r}$. However, this limitation is typically well above the maximum frequency of the measured signal. A better option is to limit the bandwidth based on the maximum frequency that is generated in the traveling wave from the shape of the magnetic field.

The delay function can then be divided into N number of bands, where N is an arbitrary filter order and each band has an integral of 2π. Obtaining a good fit at lower frequencies is often achieved by adding a constant delay, δ_0, to the entire delay function. The constant delay can also be defined so that the integral of $\delta(\omega) > 2\pi N$ and the order of the filter is sufficient to cover the desired range of frequencies, see Fig. 1. Allpass filters with real coefficients can be achieved by specifying N to be even and centering the first band on DC and the last band on 2π. Then the first and last bands have an integral of π and the center bands have an integral of 2π. Following this, the center bands can be combined as complex conjugate pairs to form biquads having real coefficients [6].

The design process presented here is similar to the process summarized in [6] and is the design procedure of the allpass filter:

1) Add a constant delay and define the filter order N.

2) Starting at DC, divide $\delta(\omega)$ into 2π area frequency bands, but have the first and last band be π area bands. The pole frequencies are then the band midpoints, $\theta = (\omega_+ + \omega_-)/2$.

3) Fit a first-order (complex) allpass section $G_n(\tilde{z})$ to each band.

4) Cascade the first order sections to form the allpass filter. The first and last sections remain first order and the others form biquad pairs, Fig. 2.

978-1-5386-3383-0/17/$31.00 ©2017 IEEE

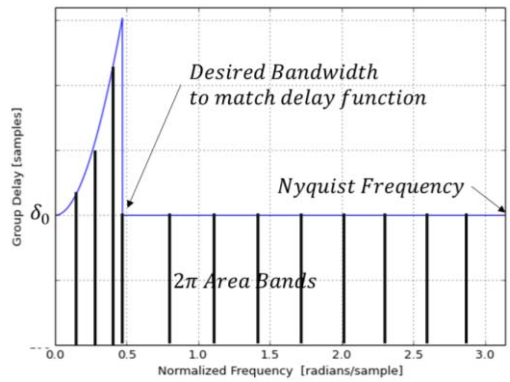

Fig. 1. A sample desired delay function and the segmentation of the function into areas of 2π after adding a constant delay.

The pole radius is chosen so that the group delay of each filter is a fraction β of the peak delay at the band edges. Thus allowing for a smoother fit of the desired group delay and the radius becomes a function of β,

$$\rho(\beta) = \alpha - (\alpha^2 - 1)^{1/2} \tag{8}$$

Where $\alpha = \frac{1-\beta\cos\Delta}{1-\beta}$ *and* $\Delta = \frac{\omega_+ - \omega_-}{2}$

The design method is robust and allows for the creation of very high order allpass filters. There is considerable flexibility in the method as the delay function, filter coefficients, and β can be updated on-the-fly as the signal is processes point-by-point. The parameter β can also be a function of ω. Other correction effects could also be added to the process fairly easily, such as frequency dependent attenuation.

C. Pulse Width Correction

In the case where the magnetic field is not uniform over the region of interest the pulse width is set so the product of the wave speed and the pulse width, $c_0\Delta t$, is less than the length over which the field varies. However, the tradeoff is the averaging effect of the longer pulse duration on the measured signal. During the time that the wave is traveling and the current is still on, there is an averaging or convolution of the magnetic field first integral with the rectangular window function. Convolution in the time domain is multiplication in the frequency domain, so if $\widehat{U}(\omega)$ is the Fourier transform of the measured signal and $G(\omega)$ is the Fourier transform of the rectangular window then the displacement without averaging, $U(\omega)$, can be recovered by dividing in the frequency domain

$$U(\omega) = \frac{\widehat{U}(\omega)}{G(\omega)} \tag{9}$$

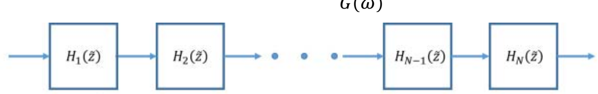

$$G_1(\tilde{z}) = \frac{-\rho_1 e^{j\theta_1} + \tilde{z}^{-1}}{1 - \rho_1 e^{j\theta_1}\tilde{z}^{-1}} \quad G_n(\tilde{z}) = \frac{(-\rho_n e^{j\theta_n} + \tilde{z}^{-1})}{(1 - \rho_n e^{j\theta_n}\tilde{z}^{-1})}\frac{(-\rho_n e^{-j\theta_n} + \tilde{z}^{-1})}{(1 - \rho_n e^{-j\theta_n}\tilde{z}^{-1})} \quad G_N(\tilde{z}) = \frac{-\rho_N e^{j\theta_N} + \tilde{z}^{-1}}{1 - \rho_N e^{j\theta_N}\tilde{z}^{-1}}$$

Fig. 2. Cascaded all pass filter. The first and last filter sections consist of a single real pole and the center sections combine to form biquads from a complex conjugate pair yielding real coefficient filters.

Then u(t) can be recovered by using the inverse Fourier transform on $U(\omega)$.

It should be noted that $G(\omega)$ goes to zero at frequencies that are multiples of f_s/N, where $N = f_s\Delta t$ is the number of data samples in the moving average and f_s is the sampling frequency. This creates issues when performing the deconvolution. Resolution of this can be solved by limiting the number of frequency components to be used for the deconvolution of the signal to be less than f_s/N or a constant can be added to $G(\omega)$ to prevent the division by zero.

IV. Measurement Results and Discussion

A. Measurement Setup

Measurements were performed in the magnetic measurement laboratory at the Advanced Photon Source at Argonne National Laboratory. Because of its tensile strength and conduction properties, uninsulated Beryllium Copper (BeCu) wire with a diameter of 75 µm was used. The 635 nm laser source, model MCLS1, was directed at a 40 µm slit, model S40R, and the intensity of the laser light was sensed by a photodiode, model SM05PD2A, which was connected to a photodiode amplifier, model PDA200C, that output a voltage proportional to the detected light. Mounting the laser-photodiode arrangement on a stage allowed the sensor to be positioned so that the wire blocked half of the 40 µm slit when at rest. The wire was attached to stages that were placed 4.8 m apart and a tension of around 2 N was applied to the wire by moving the stages. An illustration of the setup is shown in Fig. 3.

B. Wave Speed Measurement

The setup to measure the wave speed is shown in Fig. 3. Two permanent magnets separated by a small gap were used to create the reference magnetic field and the shape of the first integral of the magnetic field was designed to create a wide band of frequency components, i.e. a tall narrow pulse. The reference magnet was placed at two distances, z1 and z2, with a difference of Δz , from the photodiode sensor that measures the displacement of the wire during a measurement. Following the procedure for calculating the wave speed as a function of frequency resulted in setting the fit parameter, a, in (1) to be 1.07. The measured value of this term for this wire was 2.08E-7 N-m^2 which is similar to the value calculated with the listed properties of BeCu wire. The plot of the wave speed versus frequency is shown in Fig. 4 where it can be seen that the higher frequency components of the wave travel faster than the lower frequency components.

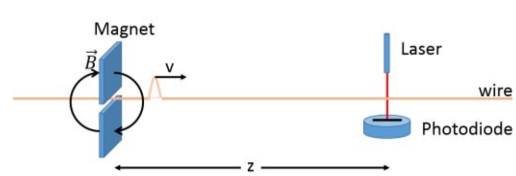

Fig. 3. Setup of the pulsed wire measurement with two magnets to create the reference magnetic field.

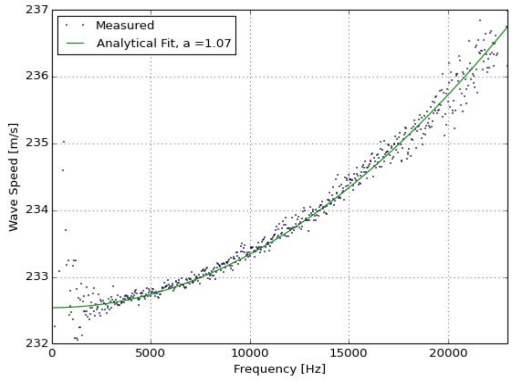

Fig. 4. The wave speed as a function of frequency of 75 µm beryllium copper wire used in the experiment. The 4.8 m long wire was tensioned to approximately 2 N for this measurement.

C. Reference Magnet Measurement

The reference magnet was measured again at various distances from the sensor and the correction algorithms for dispersion and the pulse width were verified. Fig. 5 is the raw voltage measurement of the output of the photodiode amplifier of the reference magnet at three distances from the photodiode. The effects of dispersion are clearly noticeable as the magnet is placed further from the sensor.

Using the results of the wave speed measurement and the all pass filter design method, the dispersion correction was implemented. The sampling frequency was 500 kHz and the group delay function was updated every 100 data points. In order to achieve a good match to the desired delay function of a band of frequencies equal to 0.2 × Nyquist frequency, a filter of order 100 with a β equal to 0.85 and δ_0 equal to 200 was created.

The dispersion correction and pulse width correction algorithms were applied to the reference magnet measurements at the three different locations. The results are shown in Fig. 6.

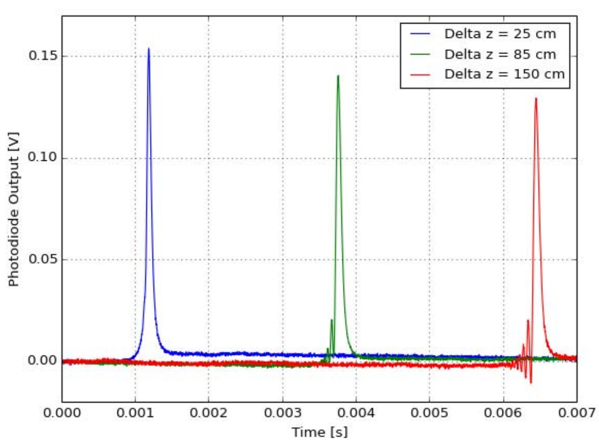

Fig. 5. Raw sensor data of the reference magnet measured at different locations.

V. Conclusion

A method for correcting the influences of dispersion and the pulse width when using the pulsed wire method to measure a magnet have been described. The correction method utilizes digital signal processing techniques and provides flexibility to the correction method. A small reference magnet was measured using the pulsed wire method. The correction algorithm was applied to these measurements and the results were compared to the Hall probe measurement data.

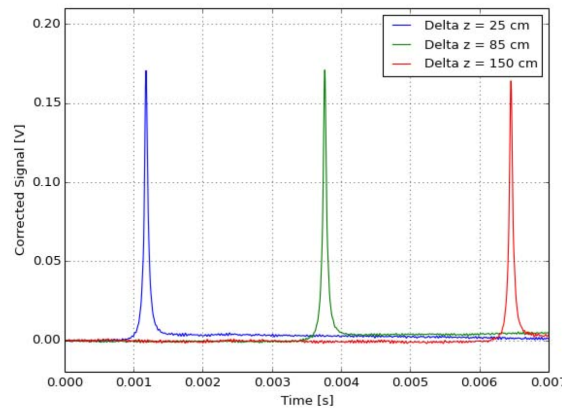

Fig. 6. Results of the pulsed wire measurements at different locations of the reference magnet after correction.

Acknowledgment

The authors wish to thank Efim Gluskin for his encouragement, guidance, and support throughout the process of completing this work. Alexander Zholents and Yury Ivanyushenkov for providing valuable guidance and discussions. Diego Arbelaez for the introduction to the pulsed wire technique and valuable discussions along the way. Also, Charles Doose for always being willing to assist and be patient with questions.

References

[1] R. W. Warren, "Limitations on the Use of the Pulsed Wire Field Measuring Technique", *Nucleear Instruments and Methods in Physics Research Section A: Accelerators, Spectrometers, Detectors and Associated Equipment*, vol. 272, no.1-2, pp. 257-263, 1988.

[2] T. C. Fan, F. Y. Lin, C. S. Hwang and I. C. Hsu, "Pulsed Wire Magnetic Field Measurements on Undulator U10P," *2001 Particle Accelerator Conference*, pp. 2775-2777, 2001.

[3] V. Kumar, G. Mishra, "Analysis of Pulsed Wire Method for Field Integral Measurements in Undulators", *Pramana - Journal of Physics*, vol. 74, no. 5, pp. 743-753, 2010.

[4] D. Arbelaez, et al., "A dispersion and pulse width correction algorithm for the pulsed wire method", *Nucleear Instruments and Methods in Physics Research Section A: Accelerators, Spectrometers, Detectors and Associated Equipment*, vol. 716, pp. 62-70, 2013.

[5] G. Sharma, G. Mishra and Mona Gehlot, "Analysis of Pulsed Wire Measurements on Bi-harmonic Undulator", *Measurement*, vol. 82, pp. 334-344, 2016.

[6] J. S. Abel and J. O. Smith, "Robust Design of Very High-Order Allpass Dispersion Filters", *Proceedings of the 9th International Conference on Digital Audio Effects*, Montreal, Canada, September 18-20, 2006

[7] J. O. Smith, "Physical Audio Signal Processing: for Virtual Musical Instruments and Audio Effects", W3K Publishing, 2010. pp. 545-546.

[8] P.M. Morse, "Vibration and Sound", McGraw-Hill Book Company Inc., 1948

978-1-5386-3383-0/17/$31.00 ©2017 IEEE